Heat and Mass Transfer (2019) 55:2165–2171
https://doi.org/10.1007/s00231-019-02575-4

ORIGINAL

Mass transfer determination of ethanol adsorption on activated carbon: kinetic adsorption modeling

Meysam Hajilari[1] · Ahmad Shariati[1] · Mohammadreza Khosravi-Nikou[1]

Received: 28 August 2018 / Accepted: 22 January 2019 / Published online: 28 January 2019

Abstract

In present work, the batch kinetic adsorption of ethanol on a commercial activated carbon was experimentally investigated and mathematically modeled in order to estimate effective diffusion and average film mass transfer coefficients. The effects of adsorbent loading, ethanol initial concentration and adsorbent particle size were studied. Two kinetic models were fitted to the experimental data. The results showed that the adsorption of ethanol on activated carbon is controlled by pore diffusion resistances. In addition, results showed that with increasing the initial concentration of ethanol in the bulk phase, the effective diffusion mass transfer slightly increased. Increasing the particle size and adsorbent loading slightly decreased the effective diffusion mass transfer. The average film mass transfer coefficient was increased by increasing initial ethanol concentration and decreased by increasing particle size and adsorbent loading. The estimated effective diffusion mass transfer coefficient was in the range of 2.47-3.17 × 10^{-10} m^2/s and average film mass transfer coefficient was in the range of 2.11-2.44 × 10^{-6} 1/s for different experimental conditions.

Nomenclature

A	Total external surface area of all adsorbent particles (m^2/g)
C	Intraparticle diffusion constant related to the boundary layer thickness (g/g)
C_0	Initial concentration of ethanol added to the vessel (kg/m^3)
C_b	Solute bulk concentration (kg/m^3)
C_i^{cal}	Estimated concentration from the model (kg/m^3)
C_i^{exp}	Experimental concentration (kg/m^3)
$C_{P\|r=Rp}$	Solute concentration at the surface of the adsorbent (kg/m^3)
C_t	Ethanol concentration in time t (kg/m^3)
D_{eff}	Effective diffusivity that incorporated pore and surface diffusion (m^2/s)
$J\|_R$	Rate of mass transfer into the particles
K	Langmuir isotherm constant (m^3/kg)
K_f	Average film mass transfer (m/s)
k_{id}	Intraparticle diffusion rate constant (g g^{-1} $min^{-0.5}$)
m_a	Mass of activated carbon adsorbent added to the vessel (g)
m_s	Volume of the initial solution (m^3)
N_{exp}	Number of experimental data points
q	Rate of adsorption that takes place on the adsorbent (g/g)
q_m	Langmuir isotherm constant (g/g)
q_t	Amount of solute adsorbed at time t (g/g)
r	Radial direction (m)
Rp	Particle radius (m)
t	Time (s)
V	Volume of the vessel (m^3)

Greek symbols

α	Is the exterior particles surface area per volume of pellet (m^2 external area/m^3 particles)
ρ_a	Adsorbent density (kg/m^3)
ε	Bed porosity

1 Introduction

Liquid phase adsorption of bioethanol from the effluent of the fermentation process is a promising technique for production of fuel-grade bioethanol and reducing cost and energy requirement of the process [1–5]. Development of such process requires precise knowledge of adsorption phenomena that occurs inside the adsorbents particles and also the dynamics of flow inside of the packed bed column [2]. Adsorption isotherm, overall mass transfer, and kinetics of adsorption have

✉ Ahmad Shariati
shariati@put.ac.ir

[1] Gas Engineering Department, Ahwaz Faculty of Petroleum, Petroleum University of Technology, Ahwaz, Khozestan, Iran

a key role in developing such processes [3, 6, 7]. The overall mass transfer coefficient can be determined from theoretical and empirical correlations to some extent but not always accurate. Estimation of overall mass transfer coefficient from mathematical correlations for dynamic ethanol adsorption on silicalite [8], activated carbon [4, 9] and a polymeric resin [10] in a fixed bed column are presented in the literature. However, some researches have been conducted to determine overall mass transfer coefficient of water and ethanol in vapor phase adsorption into activated carbon and zeolites [11–13] while a few researches have been conducted to estimate the overall mass transfer coefficient of ethanol into different adsorbents in liquid phase [1, 3, 7, 14]. Modeling of experimental batch adsorption kinetic on calcined Na-ZSM5 [14], and activated carbon [3, 15] were reported in the literature. The overall mass transfer coefficient that obtained from experimental batch kinetic data was subjected to the assumptions of pore or surface diffusion of ethanol into the adsorbent pores while in reality, both surface and pore diffusion have attributed to the mass transfer mechanism and must be considered in the modeling of batch kinetic of adsorption.

Therefore, in this study, the mass transfer coefficients of ethanol adsorption on activated carbon are determined by using experimental batch adsorption data that are fitted to mathematical kinetic models. In order to validate the results, they were compared with similar available data in literature.

2 Experimental procedure

2.1 Reagents

Activated carbon was purchased from Chem-LAB®. Ethanol (99.99 wt%) was purchased from SAMCHON Co..

2.2 Kinetic ethanol adsorption procedure

The activated carbon used in this study is charcoal base and properties of this adsorbent are presented in Table 1.

The activated carbon has particle sizes in range of 0.2 to 3 mm. In this study, adsorbent particles were meshed and separated in different particle sizes. For each experiment, a predetermined amount of adsorbent placed in a vial at the thermos-stated bath with magnet stirring. Then 10 g (±0.002 g) of ethanol/water mixture was introduced into the vial and stirred. At specific intervals about 2 μL of the sample was driven from the vial and then analyzed by gas chromatograph (FID detector, Yinglin 6100 series).

The amount of adsorbed ethanol is calculated according to the following equation:

$$q_t = \frac{m_s(C_0 - C_t)}{m_a} \tag{1}$$

where q_t is the amount of ethanol adsorbed in time t, m_s is the volume of the initial solution, C_0 is the initial concentration of ethanol added to the vessel, C_t is the ethanol concentration in time t, m_a is the amount of activated carbon adsorbent added to the vessel. The mass of the solution in contact with adsorbent assumed to be constant due to the very small amount of solution taken for concentration analysis.

2.3 Mathematical modeling of kinetic of adsorption

2.3.1 Pore diffusion model

Mathematical modeling of a batch adsorption system includes diffusion of solute from bulk phase to the surface of the adsorbent particle, the intraparticle diffusion of solute molecules into the adsorbent pores and also adsorption of the solute into the surface of the solid [16]. Different formulations were proposed for adsorption inside the particles pores based on the adsorption mechanism such as pore diffusion, surface diffusion and pore and surface diffusion [16].

Solute mass balance in bulk phase Due to the constant total amount of solute in the batch vessel, the rate of mass change of solute in liquid balk is equal to the amount of mass adsorbed into the adsorbent particles. This can be expressed as eq. (2):

$$V\frac{\partial C_b}{\partial t} = -AJ\Big|_R \tag{2}$$

where V is the volume of the vessel, C_b is the solute bulk concentration, t is time, A is the total external surface area of all adsorbent particles and $J|_R$ is the rate of mass transfer into the particles. For homogenous size and spherical particles, eq. (2) can be written in the form of eq. (3) [3]:

$$\frac{\partial C_b}{\partial t} = -\frac{1-\varepsilon}{\varepsilon}K_f\alpha\left(C_b - C_p\big|_{r=Rp}\right) \tag{3}$$

Table 1 The properties of the activated carbon adsorbent

properties	Surface area [m^2]	Particle diameter [mm]	Average pore diameter [nm]	Pore volume [cm^3/g]
Chem-LAB ® activated carbon	925	0.2-3	1.56	0.32

where ε is the bed porosity, K_f is the average film mass transfer, $C_{P|r=Rp}$ is the solute concentration at the surface of the adsorbent and $\alpha$is the exterior particles surface area per volume of pellet (m^2 external area/m^3 particles).

Solute mass balance inside the adsorbent pore Inside the pores, mass transfer occurs by pore and surface diffusion. In order to account for both phenomena, the following equation is proposed [17]:

$$\varepsilon \frac{\partial C_p}{\partial t} = D_{eff}\left(\frac{1}{r^2}\frac{\partial}{\partial r}\left(r^2\frac{\partial C_p}{\partial r}\right)\right) - \rho_a(1-\varepsilon)\frac{\partial q}{\partial t} \tag{4}$$

where D_{eff} is effective diffusivity that incorporated pore and surface diffusion, ρ_a is the adsorbent density and the q is the rate of adsorption on the surface of the pores.

The rate of adsorption can be related to the C_p according to an isotherm model such as Langmuir or Freundlich. However, it is shown that Langmuir isotherm predicted experimental isotherm data better than Freundlich isotherm [4]. Therefore, in this study, the Langmuir isotherm was employed as follows:

$$q = \frac{q_m K C_p}{1 + K C_p} \tag{5}$$

where K and q_m are isotherm constants. If adsorption reaction occurs so rapidly, the pore diffusion becomes the rate controlling step and the adsorption can be assumed instantaneous. By local equilibrium assumption, one can write the following expression [3, 12, 13, 17]:

$$\frac{\partial q}{\partial t} = \frac{\partial q}{\partial C_p}\frac{\partial C_p}{\partial t} \tag{6}$$

By applying Langmuir isotherm as stated in eq. (5), the following equation can be derived:

$$\frac{\partial q}{\partial t} = \frac{K q_m}{\left(1 + K C_p\right)^2}\frac{\partial C_p}{\partial t} \tag{7}$$

Substituting eq. (7) into eq. (4) yields following expression:

$$\left[\varepsilon + \rho_a(1-\varepsilon)\frac{b q_m}{\left(1 + b C_p\right)^2}\right]\frac{\partial C_p}{\partial t} = D_{eff}\left(\frac{1}{r^2}\frac{\partial}{\partial r}\left(r^2\frac{\partial C_p}{\partial r}\right)\right) \tag{8}$$

Equation (3) only needs one initial condition and eq. (8) is subjected to one initial and two boundary conditions. The initial and boundary conditions for these equations are presented as follows:

$$@t = 0; C_b(0) = C_0 \ , \quad C_p(r,0) = 0 \tag{9}$$

$$\left.\frac{\partial C_p}{\partial r}\right|_{r=0} = 0 \tag{10}$$

$$-D_{eff}\left.\frac{\partial C_p}{\partial r}\right|_{r=R_p} = K_f\left(C_b - C_p|_{r=R_p}\right) \tag{11}$$

2.3.2 Intraparticle diffusion

The intraparticle diffusion model can determine the possibility of intraparticle diffusion resistance that may affects the adsorption process [18]. This model is expressed as follows:

$$q_t = k_{id}.\sqrt{t} + C \tag{12}$$

where the q_t is the amount of solute adsorbed at time t, k_{id} is the intraparticle diffusion rate constant (g g^{-1} $min^{-0.5}$) and C is a constant related to the boundary layer thickness (g/g).

2.3.3 Numerical solution

Due to the nonlinearity of the model equations a numerical solution was employed. The pore diffusion model equations (i.e. equations (3) and (8)) with related initial and boundary conditions (eqs. (9), (10) and (11)) were solved by the method of lines (MOL). In this method, the time derivatives remain continuous while the spatial derivatives are discretized by finite difference method. This will convert partial differential equation to a set of ordinary differential equations (ODE's). In this study, the eq. (8) was converted to a system of ODE's and coupled with the other ODE (eq. (3)) in the model. Then, this system of ODE's was solved by ode15s solver in MATLAB software. Initial and boundary conditions were used for solving this set of equations.

In this study, the effective diffusivity (D_{eff}) and average film mass transfer K_f are unknown. These parameters are estimated by fitting the model to experimental concentration data.

In order to estimate model parameters from experimental data, the following objective function was employed:

$$OF = \frac{1}{N_{\exp}}\sum_{i=1}^{N_{\exp}}\left|\sqrt{\left(C_i^{\exp} - C_i^{cal}\right)^2}\right| \tag{13}$$

where N_{exp} is the experimental data points, C_i^{exp} is the experimental concentration and C_i^{cal} is estimated concentration from the model. In this work, non-linear least square algorithm in MATLAB (lsqnonlin algorithm) was used to fit the model to the experimental data. The average absolute relative deviation (AARD) was used to calculate the error of fitting and it is presented as:

$$AARD\% = \frac{1}{N_{\exp}}\sum_{i=1}^{N_{\exp}}\left|\frac{C_i^{\exp} - C_i^{cal}}{C_i^{\exp}}\right| \times 100 \tag{14}$$

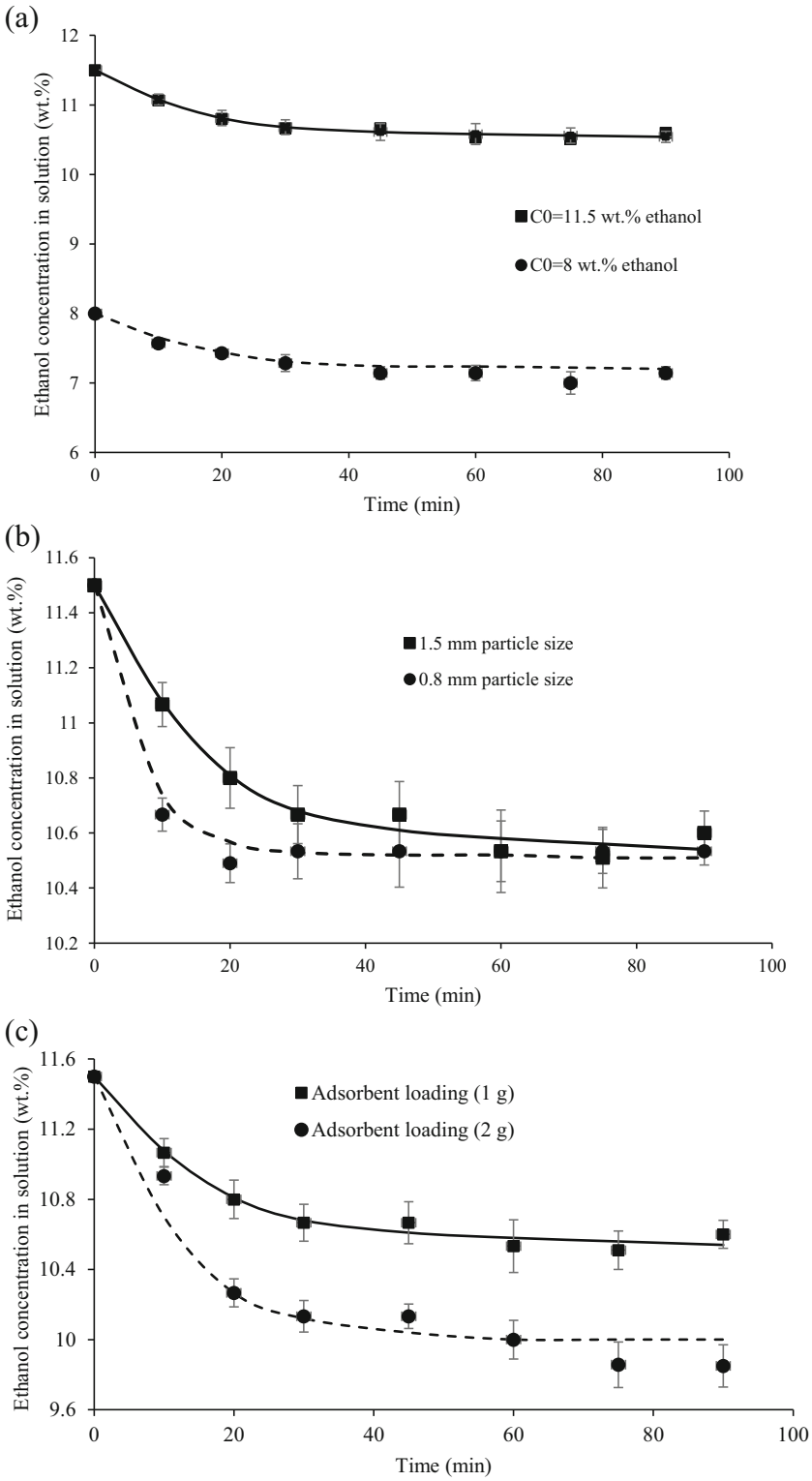

Fig. 1 Experimental kinetic adsorption data at **a** two different initial concentrations **b** two different particle sizes **c** two different adsorbent loadings. The symbols are experimental data and the solid and dashed lines are model prediction

3 Results and discussion

The kinetic adsorption experiments were conducted at ambient temperature and atmospheric pressure. The effects of adsorbent loading, ethanol initial concentration and adsorbent particle size were studied. The variation of concentration with time in the batch adsorption system is presented in figs. 1a to 1c. The error bars on the Fig. 1 represents the standard deviations of three or more concentration measurements.

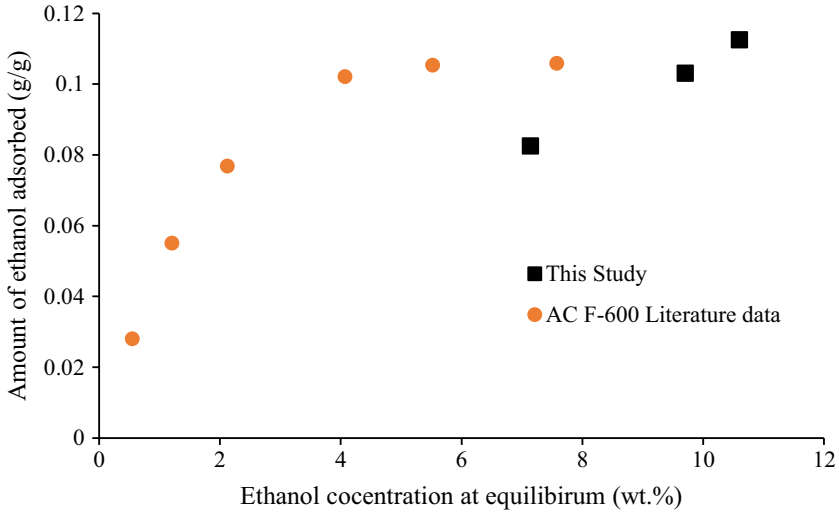

Fig. 2 The amount of ethanol adsorbed at equilibrium concentrations from batch kinetic data compared with literature data for activated carbon F-600

Figure 1a shows the effect of initial concentration of ethanol at fixed values of 1 g adsorbent loading and 1.5 mm particle size. As Fig. 1a shows, with reducing the initial ethanol concentration from 11.5 to 8 (wt.%) the decay in concentration become slower. It can be explained that as the initial ethanol concentration reduces, the saturation of active sites become slower due to lower mass transfer gradient in the system. As it can be seen, at first, a rapid decrease in the concentration occurs then declines slowly. It can be attributed to the fact that, at the beginning of the adsorption process, the adsorption sites are easily available for ethanol molecule to adsorb on the adsorbent, but as time passes, more sites occupied, the available adsorption sites become less, therefore the concentration decay till the saturation of all adsorption sites.

The effect of particle size is shown in Fig. 1b. The initial ethanol concentration was 11.5 wt.% and adsorbent loading was 1 g (±0.001 g). As it can be seen, with reducing the particle size, the rapid decrease in ethanol concentration in bulk becomes more pronounced. It is evident that by reducing the particle size, the diffusion resistance decreases and active sites for adsorption become more easily available. The time required to reach the same equilibrium concentration for larger particles is much higher than that for smaller particles.

In Fig. 1c, the effect of adsorbent loading on concentration change in the solution is shown. The initial concentration was 11.5 wt.% and the average particle size was 1.5 mm. As it can be seen, by increasing the amount of adsorbent, the change in the concentration is more pronounced which indicates higher ethanol molecule adsorbed on the adsorbent which is as expected.

From concentration data in the kinetic model, the amount of ethanol adsorbed at equilibrium concentrations are plotted in Fig. 2. The data are compared with literature equilibrium isotherm data.

As results shown in Fig. 2, the equilibrium data in this work are comparable with literature data for similar commercial activated carbon [3]. In this case, the F-600 showed higher adsorption capacity at lower concentration, but at higher concentration,

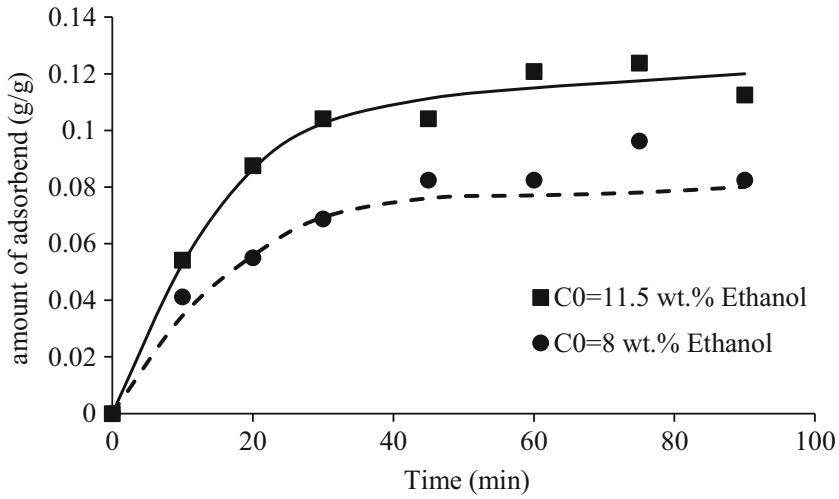

Fig. 3 Amount of ethanol adsorption with time. The symbols represent the experimental data. The solid and dashed lines represent model predictions

Table 2 The experimental kinetics runs and fitted parameters of the pore diffusion model

Experimental Run #	Initial ethanol concentration (wt.%)	Particle diameter (mm)	Adsorbent loading (g/ 10 ml solution)	D_{eff} (m^2/s)	K_f (1/s)	AARD (%)
1	11.53	1.5	1	2.89×10^{-10}	2.25×10^{-6}	4.25
2	11.50	1.5	2	2.63×10^{-10}	2.11×10^{-6}	4.8
3	8.02	1.5	1	2.47×10^{-10}	2.03×10^{-6}	3.82
4	11.50	0.8	1	3.17×10^{-10}	2.44×10^{-6}	5.21

it is comparable with Chem-Lab® activated carbon. At higher ethanol concentration, the amount of ethanol adsorption in this work is higher. The amount of ethanol adsorption with time at different concentration is presented in Fig. 3.

The data in Fig. 3 are fitted for initial concentration effect. The trend for effects of adsorbent loading and particle size are similar. By fitting the kinetic pore diffusion model to the experimental kinetic adsorption data, the model parameters were determined. The fitted parameters of the pore diffusion model are presented in Table 2. As the results show, with increasing the particle diameter the effective diffusivity decreased and in a similar manner, the average film mass transfer is also decreased. In addition, by reducing the initial concentration from 11.5 to 8 wt.% the effective diffusivity and average film mass transfer also decreased, however, the variation is less than 10%.

The estimated values for effective diffusivity in this study are in the same order with the values that have been reported in literature. Jones et al. estimated an average effective diffusivity of 3.8×10^{-10} m^2/s for ethanol adsorption on F-600 activated carbon in similar experimental procedure [3]. A value of 3.45×10^{-9} (m^2/s) to 5.52×10^{-9} (m^2/s) for vapor ethanol in three different activated carbon adsorbents were reported elsewhere [13].

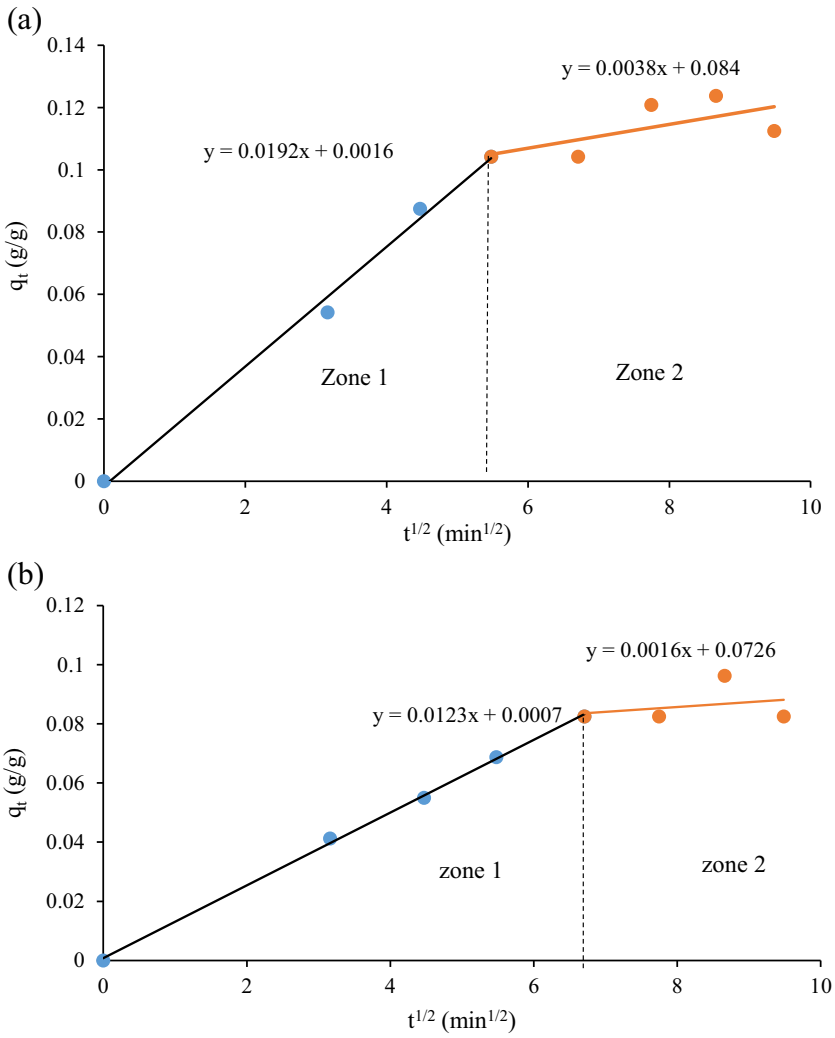

Fig. 4 Intraparticle diffusion model results for **a** C_0 = 11.5 wt.% and **b** C_0 = 8 wt.%

The AARD% of the fitted model to experimental data shows that the model can predict the data very well. The estimated values from these kinetic experiments can be used for designing and simulation of fixed bed adsorption column.

The intraparticle diffusion model is fitted to the experimental data and the results are presented in Fig. 4. According to intraparticle diffusion model, the plot of q_t versus $t^{1/2}$ must be a straight line when intraparticle diffusion reticence is rate controlling step of adsorption phenomena. Figure 4a and b, shows a multi-linear plot of q_t versus $t^{1/2}$. This type of multi-linear plot means that different steps of adsorption on the adsorbent surface are occurred [18]. Therefore, it is evident that the adsorption of ethanol on activated carbon is not intraparticle diffusion controlled.

From Fig. 4, first step (zone 1) is assigned to pore diffusion of the ethanol molecules to the adsorbent pore and the second step (zone 2) related to the adsorption of ethanol molecule inside smaller pores [19]. Therefore, the intraparticle mass transfer resistance for ethanol adsorption on commercial activated carbon is not a rate controlling step. However, as it is shown in Fig. 3, the pore diffusion model was fitted to experimental data very well, that suggests the mechanism that describe this model controls adsorption of ethanol on activated carbon in liquid phase.

4 Conclusion

In this study, the experimental batch kinetic data was mathematically modeled to determine the effective mass transfer diffusion of ethanol from the liquid phase into activated carbon adsorbent. Effects of adsorbent particle size, initial ethanol concentration and adsorbent loading on the kinetics were investigated. The particle size and adsorbent loading have the reverse effects on effective diffusivity while the initial concentration has a direct effect on effective diffusivity. The average film mass transfer is also increased by increasing the ethanol concentration in the bulk and decreased by increasing in particle size and adsorbent loading. The pore diffusion and intraparticle diffusion models were fitted to experimental data, the results suggest that the mechanism described the pore diffusion model may control adsorption of ethanol on activated carbon in liquid phase.

References

1. Fujita H, Qian Q, Fujii T et al (2011) Isolation of ethanol from its aqueous solution by liquid phase adsorption and gas phase desorption using molecular sieving carbon. Adsorption 17:869–879. https://doi.org/10.1007/s10450-011-9354-2
2. Rao MB, Sircar S (1992) Production of Motor Fuel Grade Alcohol by Concentration Swing Adsorption. Sep Sci Technol 27:1875–1887. https://doi.org/10.1080/01496399208019455
3. Jones RA, Thibault J, Tezel FH (2010) Simulation and validation of ethanol removal from water in an adsorption packed bed: Isotherm and mass transfer parameter determination in batch studies. Can J Chem Eng 88:889–898. https://doi.org/10.1002/cjce.20337
4. Hajilari M, Shariati A, Nikou MK (2018) Equilibrium and dynamic adsorption of bioethanol on activated carbon in liquid phase. Chem Eng Technol. https://doi.org/10.1002/ceat.201800219
5. Hajilari M, Shariati A, Khosravi-Nikou M (2018) Equilibrium adsorption of bioethanol from aqueous solution by synthesized silicalite adsorbents: experimental and modeling. Adsorption. https://doi.org/10.1007/s10450-018-9992-8
6. Farhadpour FA, Bono A (1996) Sorption separation of ethanol-water mixtures with a bi-dispersed hydrophobic molecular sieve, silicalite: measurement and theretical analysis of column dynamics. Chem Eng Process 35:157–168
7. Farhadpour FA, Bono A (1988) Adsorption from solution of non-electrolytes by microporous crystalline solids: Ethanol-water/silicalite system. J Colloid Interface Sci 124:209–227. https://doi.org/10.1016/0021-9797(88)90341-4
8. Delgado JA, Uguina MA, Sotelo JL et al (2012) Separation of ethanol – water liquid mixtures by adsorption on silicalite. Chem Eng J 180:137–144. https://doi.org/10.1016/j.cej.2011.11.026
9. Delgado JA, Águeda VI, Uguina MA et al (2015) Separation of ethanol – water liquid mixtures by adsorption on BPL activated carbon with air regeneration. Sep Purif Technol 149:370–380. https://doi.org/10.1016/j.seppur.2015.06.011
10. Delgado JA, Águeda VI, Uguina MA et al (2013) Separation of ethanol – water liquid mixtures by adsorption on a polymeric resin Sepabeads 207. Chem Eng J 220:89–97. https://doi.org/10.1016/j.cej.2013.01.057
11. Simo M, Brown CJ, Hlavacek V (2008) Simulation of pressure swing adsorption in fuel ethanol production process. Comput Chem Eng 32:1635–1649. https://doi.org/10.1016/j.compchemeng.2007.07.011
12. Yamamoto T, Kim YH, Kim BC et al (2012) Adsorption characteristics of zeolites for dehydration of ethanol: Evaluation of diffusivity of water in porous structure. Chem Eng J 181–182:443–448. https://doi.org/10.1016/j.cej.2011.11.110
13. Bouzid M, Ben Torkia Y, Wjihi S, Ben Lamine A (2017) Kinetic adsorption modeling of ethanol molecules onto three types of activated carbons: Microscopic interpretation of adsorption and diffusion parameters. J Mol Liq 242:98–108. https://doi.org/10.1016/j.molliq.2017.06.066
14. Falamaki BC, Sohrabi M, Talebi G (2001) The Kinetics and Equilibrium of Ethanol Adsorption from Aqueous Phase Using Calcined (Na-1 , 6-Hexanediol) -ZSM-5. Chem Eng Technol 24:501–506. https://doi.org/10.1002/1521-4125
15. Besedova E, Bobok D (2003) Adsorption of ethanol on activated carbon. Chem Pap Zvesti 57:27–34
16. Do DD (1998) Adsorption Analysis: Equilibria and Kinetics. Published by Imperial College Press and distributed by World Scientific Publishing Co.
17. Maria ME, Mansur MB (2016) Mathematical modeling of batch adsorption of manganese onto bone char. Braz J Chem Eng 33:373–382. https://doi.org/10.1590/0104-6632.20160332s20140077
18. Lima ÉC, Adebayo MA (2015) Carbon Nanomaterials as Adsorbents for Environmental and Biological Applications. Springer International Publishing, Cham
19. Machado FM, Bergmann CP, Lima EC et al (2012) Adsorption of Reactive Blue 4 dye from water solutions by carbon nanotubes: experiment and theory. Phys Chem Chem Phys 14:11139. https://doi.org/10.1039/c2cp41475a